Chapter 1

Introduction

1.1 Statistical mechanics and its evolution

Statistical mechanics is a branch of physics which utilizes methods of probability theory and statistics. Statistical mechanics is a tool that can be applied to almost all physical systems irrespective of the laws the system obeys. Laws of statistical mechanics are always valid even if old ones replaced new laws, natural laws modified to deeper laws by approximation, and if new laws are discovered, it will be valid on them too as it works on old ones. Statistical mechanics was started to be developed at the end of the nineteenth century with the primary works of Ludwig Boltzmann, who personally published more than a hundred papers throughout his life [Uffink (2017)]. Other scientists like James Clerk Maxwell [Grant & Phillips (2013)], Josiah Willard Gibbs [Klein (1990)], and Albert Einstein [Sen (2021)] played a significant role in the formulation of it. It grew from the thermodynamics that describes the mysterious behavior of materials called heat or caloric. Thermodynamics involves natural laws discovered by the experiments; however, heat is an emergent phenomenon: there should be mathematical formulation defined in terms of a more detailed analysis (dynamics of individual particles); hence, later on, the laws of thermodynamics formulated in a deeper theory by applying statistical mechanics [Pathria

(1996); Zemansky & Dittman (1997)]. Statistical mechanics does not care about the details of the individual particles how they are moving. One can find that they collectively behave like a continuous fluid. That is all about statistical mechanics: deriving high-level descriptions by initializing lower descriptions and averaging lots of system details.

Up to now, we understood that statistical mechanics deals with a deeper degree of freedom and aims to make a connection between the macroscopic properties to the microscopic properties of matter in the thermodynamic equilibrium [Pathria (1996); Zemansky & Dittman (1997)], which provides the physical properties of the matter on different times and length scales by calculating the statistical fluctuations [Pathria (1996); Zemansky & Dittman (1997)]. Statistical equilibrium does not mean that particles cease their motion, rather than ensemble is not evolving. Let us first discuss the connection between thermodynamics and statistical mechanics. In thermodynamics, there are three types of thermodynamic ensembles [Pathria (1996); Zemansky & Dittman (1997)] *Microcanonical (N, E, V), Canonical (T, V, N), and Grand canonical ensemble (T, V,μ)* where N, E, V, T, and μ corresponds to the number of particles, total energy, volume, temperature and chemical potential of the system and remains fixed in their respective ensembles. Let us consider a physical system composed of N identical particles in volume V with total energy E where the macrostate of the system is defined by variable (N,E,V). On the other hand, there are various ways where the total energy of the system E can be distributed among the N particles. Since there is the various possible arrangement of the particles which is called microstates of the system [Pathria (1996); Zemansky & Dittman (1997)]. Therefore, to describe the system in three-dimensional space $(3D)$, $6N$ degrees of freedom is required. This 6N dimensional space is named as *phase space* [Pathria (1996); Zemansky & Dittman (1997)] of the system, and each point in phase space is named as phase point called microstate of the system. In contrast, the collection of a large number of microstates is known as macrostate. Since in the microscopic approach, there is a larger number of degrees of freedom; hence it is difficult to trace each microstate; hence we can define the probability dP of the system in an elemental volume dV of the phase space using statistical information. The probability dP is defined as $dP = lim_{t\to\infty}\frac{dt}{T}$, where dt represent the time spent by the system in the volume element dV and T is the total time over which system is tracked. The average of any statistical quantity $f(t)$ along a trajectory is defined by $\overline{f} = lim_{\tau\to\infty}\frac{1}{\tau}\int_0^\tau f(t)dt$ [Pathria (1996); Zemansky & Dittman (1997)]. By this approach, one can calculate the time average of any statistical quantity. Another method to calculate the average of any statistical quantity is called ensemble averaging. In this method, each phase point in the phase space is treated as different copies of the same system called an ensemble. Let $\overline{N}$ is the number of copies corresponds to the volume V, and $\overline{dN}$ is the number of copies corresponding to volume element dV, then the probability of the system being in volume V is defined as $d\overline{P} = lim_{\overline{N}\to\infty}\frac{d\overline{N}}{\overline{N}} = \rho(q_i, p_i)dV$, where q_i, p_i, and $\rho(q_i, p_i)$ are $3N$ position, momentum coordinates, and density in the phase space respectively. Average of any quantity f can be calculated by defining $< f >= \int f\rho dV$, where ρ is the probability density function [Pathria (1996); Zemansky & Dittman (1997)]. Equilibrium statistical mechanics is based on the following postulates (i) *Ergodic hypothesis* : The system that evolves with time to explore all accessible states. Both the description discussed above are identical, (ii) *apriori probability* : For a macrostate compatible with microstate, in the absence of any further information, one can assign that all microstates are equally probable. In a more elaborative version, the principle of priori states that the correct ensemble is that ensemble which is compatible with the known information and has the largest *information entropy*, and (iii) Boltzmann's hypothesis: If a trajectory fills the space by a hypervolume ω in the phase spase, then the system entropy is defined as $s = kln\omega$, where k is the Boltzmann's constant [Pathria (1996); Uffink (2017); Zemansky & Dittman (1997)]. Boltzmann's relation provides the bridge between thermodynamics and statistical mechanics while the ergodic hypothesis state that the system is internally consistent [Pathria (1996); Zemansky & Dittman (1997)].

Many of the natural systems are in general nonequilibrium; for examples *self-propelled*: fish schools [Katz et al. (2011)], bird flocks [Ballerini et al. (2008)], actin filaments [Hubbard et al. (2004)], microtubules [Sumino et al. (2012a)], colloidal rollers [Morin et al. (2017)] and autophoretic colloids [Buttinoni et al. (2013); Palacci et al. (2013); Theurkauff et al. (2012)], rheology of biological suspension [Giomi et al. (2010); Hatwalne et al. (2004); Liverpool & Marchetti (2006)], time-dependent Hamiltonian systems [Struckmeier & Riedel (2001)], etc.

In the last few decades, there has been a significant enhancement in the understanding of the different phenomena of the natural systems like collective behavior of many biological and cellular systems [Huang (1987); Suzuki et al. (1995)] as suspension of swimming bacteria [Dombrowski et al. (2004)] or other motile organism, cell suspensions, and collection of cytoskeletal filaments [Ahmadi et al. (2006)] such as microtubules [Sumino et al. (2012a); Surrey et al. (2001)] and molecular motors, such as myosin [Joanny et al. (2007); Kron & Spudich (1986); Kruse & Jülicher (2000, 2003); Kruse et al. (2001, 2004); Kruse et al. (2005)]. Understanding such nonequilibrium systems in terms of their statistical mechanics as well as the thermodynamic framework is an emerging area of current research. A nonequilibrium system arises from a wide range of situations with very different phenomenologies. One can identify those that involve sufficient ingredients to form coherent classes. One of such systems approaches towards relaxation but have not reached thermal equilibrium. The relaxation time might be fast or become extremely slow. The second class of nonequilibrium describes whose collective dynamics stop attaining equilibrium by imposing non-zero steady currents as boundary conditions. Examples of such systems are heat-flow experiments in which a piece of matter is connected with the two reservoirs held at different temperatures.

The third class of nonequilibrium systems, which is often called active matter [Bendix et al.

(2008); Dombrowski et al. (2004); Peruani et al. (2012); Rafaï et al. (2010); Sumino et al. (2012a); Surrey et al. (2001); Szabó et al. (2006)], where the energy of the total system is dissipated over the microscopic scale in the bulk so that each agent of the system has an irreversible dynamics [Cates (2012); Marchetti et al. (2013a,a); Ramaswamy (2017); Toner et al. (2005); Vicsek & Zafeiris (2012); Yates et al. (2010)]. Many such systems are studied over the past ten years, the quest for a generic description of active matter has attracted growing interest. It is reasonable to hope that self-propelled particles (SPPs), which otherwise interact via standard equilibrium forces (attraction, repulsion, alignment, etc.), might form a coherent subclass of nonequilibrium systems.

Active matter systems exhibit many collective behaviors; some of them are many bacterial contamination [Costerton et al. (2005); Flemming (2002)] which arise from biofilm formation whose early stage is triggered by controlling the density greater than a threshold density [Hall-Stoodley et al. (2004)]. Also, many studies of motile synthetic colloids directly form the nanostructures. More generally, one can extend the control over soft matter systems, whose applications range from liquid crystal displays to cosmetics and food processing industries.

1.2 Active matter system

The active matter study evolves historically, mainly by work on biological systems. These are often quite complex: For example, the rich phenomenology of bacterial suspension in the combination of their self-propulsion speed, the alignment interaction because of their rod-like shapes, and their hydrodynamic coupling of the medium where they swarm [Sokolov et al. (2007)]. In this thesis, we will emphasize the mechanics and statistics Nelson (2007); Tayler & group (2013) of living matter. The unifying characteristic of active matter systems is that they are composed of a huge number of individuals (SPPs), and have the ability to transduce their energy into systematic movement [Cates (2012); Marchetti et al. (2013a); Ramaswamy (2010a, 2017); Toner et al. (2005); Vicsek & Zafeiris (2012); Yates et al. (2010)]. Further, the interaction of the SPPs with the medium leads to a highly correlated collective motion.

All the active matter systems discussed above, each SPP moves forward at the cost of their internal energy, converted into mechanical work. In these systems, the dissipated energy is not correlated with the input one, like in equilibrium systems, viz., *Brownian motion*. Since the energy is injected at each particle level, the active systems differ from other nonequilibrium systems like a bulk fluid sheared from the top [Saracco et al. (2011); Saracco et al. (2012)] or driven diffusive systems [Balakrishnan (2021)]. However, for them, the nonequilibrium steady state can be defined in a similar fashion as for other equilibrium systems [Huang (1987); Pathria (1996)]. For the true equilibrium systems where macroscopic properties remain fixed, called *, i.e., steady state*, however, for nonequilibrium steady state (NESS), the relevant observables are defined in such a way that they remain the same with time. We can understand NESS by taking an example of a bird flock where all the agents of the flock move coherently.

Let us consider, the probability $P(S,t)$ of finding the system in a microscopic state S at time t. The time evolution of probability $P(S,t)$ is given by the master equation,

$$\frac{dP(S,t)}{dt} = \sum_{S' \neq S} \Omega(S' \to S)P(S',t) - \Omega(S \to S')P(S,t), \tag{1.1}$$

where, $\Omega(S' \to S)$ represents the rate of change of transition from configuration S' to S. In the steady state, $P(S,t)$ remains no longer function of time hence left hand side (L.H.S). of the Eq ~1.1 will vanish, and the probability $P(S,t)$ of the system going from configuration S to S' remains same as the probability $P(S',t)$ of the system going from S' to S. Hence the detailed balance of the system satisfied. However, the detailed balance condition is not satisfied for the active systems since there is a non-zero current in the steady-state.

Further, another significant feature of the active system is the density fluctuation which is much larger than usual equilibrium systems in the steady-state. Furthermore, the density fluctuation for the equilibrium system shows by standard deviation $\Delta N \propto \sqrt{N}$ provided the system remains away from the critical point, where N is the number of particles in a region of volume V. Moreover, for the active system, the density fluctuations grow faster than usual $\sqrt{N}$, in two dimensions. It can also grow as large as N in some cases [Ramaswamy et al. (2003)].

1.2.1 Types of active matter system

Active matter: with and without momentum conservation

This thesis will emphasize the large-scale collective behavior of active matter systems and characterize their properties. We also discuss the different types of active matter based on symmetry elements and conservation laws. Active systems are generally characterized into two types depending on having and not having momentum conservation, or dry and wet systems. First, we will discuss the dry active matter where there is no momentum conservation. Examples of this class includes the bacteria gliding on a rigid surface [Wolgemuth et al. (2002)], animal herds on land [Toner & Tu (1998)], or artificial ones, such as vibrated granular particles on a two-dimensional substrate [Blair et al. (2003); Kudrolli et al. (2008); Ramaswamy (2017); Ramaswamy et al. (2003); Yamada et al. (2003)]. In all examples, energy is dissipated on the substrate, which is work done by the frictional force, and leads to a violation of conservation of linear momentum. There are also some examples: highly concentrated swimming bacteria [Drescher et al. (2011)] and motor filament suspension [Liverpool (2003)] where the steric and stochastic effects could, for most purposes, overwhelm hydrodynamic interactions. Further, to interpret the aerial displays by a large group of birds, which has a much lower concentration in comparison to a bacterial suspension, long-range interactions appears negligible [Ballerini

et al. (2008)] and metric-free interactions, as investigated by [Ginelli & Chaté (2010)], may be modeled by introducing the minimal model. Furthermore, in the dry system, the only conserved quantity is the number of particles (neglecting death and birth), and the associated hydrodynamic field is the local density of active units. Moreover, individual active particles can be different in their respective shape and symmetry. Finally, the dry active matter can be modeled by overdamped Langevin dynamics assuming momentum transfer into the environment. In contrast, when it is necessary to include the hydrodynamic interaction, the dynamics of the suspending fluid can be incorporated by a description of the interaction of active particles and fluid with conserved total linear momentum. We refer to models with momentum conservation, where fluid flow is important, as “wet”. In general, the hydrodynamic interaction was neglected over the length greater than $\sqrt{\frac{\eta}{\gamma}}$, where η and γ represent the viscosity of the fluid and frictional drag coefficient.
This thesis aims to emphasize some key features of an active dry system where the number of particles in the system is the only conserved quantity.

1.2.2 Types of active particles

polar and apolar particles

Two types of particles characterize active matters agents, depending on the symmetry as (i) polar particles: head and tail can be distinguished [Couzin et al. (2005); Jolles et al. (2018); Sumpter et al. (2008)] , and (ii) apolar particles: head and tail can't be distinguished [Ahmadi et al. (2005, 2006)]. Further, polar particles can align parallel or anti-parallel to each other. Therefore, they will form either a polar ordered state with net flow velocity or an apolar ordered state with zero flow velocity, as shown in Fig1.1. Furthermore, apolar particles don't have polarity and form a nematic-ordered state, as shown in Fig.1.1. Moreover, the ordered state of polar particles is defined either by vector or by nematic order parameter, and a nematic order parameter specifies the ordered state of the apolar particles. Now, we will briefly describe the characteristics of the active polar particles or (self-propelled particles (SPPs)).

These SPPs show ubiquitous behavior during their motion, and they show collectively coherent motion when they are put in a collection. The prototype model of such aligning self-propelled particles was explained in 1995 by using a simple rule-based model in two-dimension [Vicsek et al. (1995)], renowned as the Vicsek model (VM). In the same year,

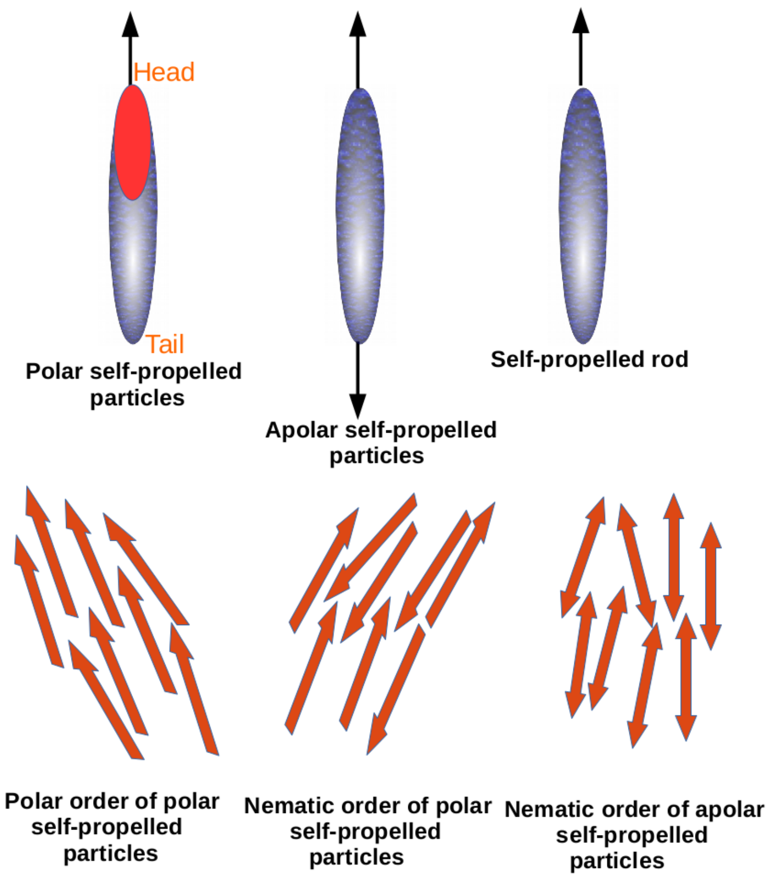

Fig. 1.1 Schematic of the various types of active particles and orientationally ordered states. Polar active particles (top left image), such as bacteria or birds, have a head and a tail and are generally self-propelled along their long axis. They can order in polar states (bottom left) or nematic states (bottom center). The polar state is also a moving state with a non-zero mean velocity. Apolar active particles (top center image) are head-tail symmetric and can order in nematic states (bottom right). Self-propelled rods (top right image) are head-tail symmetric, but each rod is self- propelled in a specific direction along its long axis. The self- propulsion renders the particles polar, but for exclusively apolar interactions (such as steric effects), self-propelled rods can order only in nematic states (bottom center).

Toner and Tu *et al.* [Toner & Tu (1995)] predicted the existence of a long-range ordered phase of flocks, in which all the SPPs of a large flock move together with a non-zero mean velocity in two dimensions (2D) [Toner & Tu (1995, 1998)].

In the Vicsek model, SPPs interact through short-range alignment interaction. The mean density of the system controls the number of SPPs, and disorder in the alignment is represented as a noise in the system. Hence the density and noise are the two main control parameters for the active system. The main result of the Vicsek model shows a nonequilibrium phase transition from a disordered state at low density or high noise to an ordered (coherent motion) state at high density or low noise strength. In the same year, Toner and Tu [Toner & Tu (1995)] reported that the flocks exhibit a true long-range order with spontaneous rotation symmetry broken in 2D, whereas there is no such symmetry broken state in 2D in equilibrium system with continuous symmetry (Mermin-Wagner theorem) [Mermin & Wagner (1966)]. For that, Toner and Tu used the hydrodynamic equations of motion for density and polarization field. Recently, the Toner and Tu model is derived by coarse-graining the microscopic Vicsek model using the Boltzmann-equation and fluctuating hydrodynamic approach [Marchetti et al. (2013a); Ramaswamy (2010a); Toner et al. (2005)]. These descriptions provide the microscopic basis for the hydrodynamic theory. Further, the system of apolar particles shows large number fluctuations in comparison to their equilibrium counterparts. The number fluctuation δN is proportional to the mean number of SPPs $< N >$ in 2D system [Ramaswamy et al. (2003)], which is known as *Giant number fluctuation*, which has been further confirmed by some experimental studies [Chaté et al. (2006); Ramaswamy (2017)]. H. Chaté *et al.* also find the existence of Kosterlitz-Thouless-like transition to quasi-long-range orientational order for apolar systems [Chaté et al. (2006)].

In the Vicsek-like systems, the particles (SPPs) are in general elongated and can align either polar or apolar (nematic) orientational order. For these systems, choice of alignment interaction plays a significant role in the formation of an ordered state. There is another interesting class of SPPs that can be distinguished from their head and tail during their motion, but they are symmetric in shape [Bialké et al. (2012); Farrell et al. (2012); Fily & Marchetti (2012); Redner et al. (2013); Solon et al. (2015b)]. This class of particles is known as Active Brownian particles (ABP). Here, simple volume exclusion will not lead to a polar/apolar ordered state. There is no alignment interaction like in the Vicsek model, and these particles do not show large-scale alignment. Further, above a packing fraction ϕ_c (smaller than ϕ_c for random close packing in 2D), this minimal system phase separates into solid-like and gas phases. Moreover, they also exhibit large number fluctuations like polar and apolar systems above the critical packing fraction ϕ_c [Fily & Marchetti (2012)]. Finally, another class of polar SPPs is often known as run-and-tumble particles, which perform self-propulsion by a sequence of runs. During these runs, they move with almost constant speed and change their direction by sudden and rapid randomization in direction or tumbles [Cates & Tailleur (2013); Solon et al. (2015c); Tailleur & Cates (2008)]. In a recent study, Tailleur et al. discuss the domain formation and other collective phenomena of these systems [Tailleur & Cates (2008)]. In this thesis, we mainly focus on polar SPPs and ABPs only.

1.3 Role of disorder or inhomogeneity among SPPs

Most of the studies in the active system have been done in the clean environments [Chaté et al. (2007, 2008); Marchetti et al. (2013a); Ramaswamy (2010a); Vicsek et al. (1995)]; however, in nature, the active system consists of different kinds of heterogeneity. In the last decades, scientists have started to look their bulk properties in heterogeneous medium [Bricard et al. (2013); Chepizhko & Peruani (2013); Chepizhko et al. (2013); Das et al. (2018); Peruani & Aranson (2018); Sándor et al. (2017); Sándor et al. (2017); Toner et al. (2018a,b)]. The study of collective properties of flocks, animal herds and swimming bacteria, etc. are crucial not only in the wild group of animals but also effective application in drug deliveries, robotics, vehicular traffic flow, population learning, biological network formation, and network theory; opinion formation and materials composed with synthetic motile units. This section will briefly discuss some of the important studies of active particles in heterogeneous mediums. In a recent study, Bialek et al. [Bialek et al. (2012)] show that the varying interaction strength of the SPPs results in maximum entropy. Hence, more information transfer among the particles [Balakrishnan (2021); Szamel (2014)]. In recent studies, the effect of different kinds of heterogeneity over the long-range behavior on collections of SPPs moving on a two-dimensional substrate [Chepizhko et al. (2013); Das et al. (2018); Toner et al. (2018a)]. It is observed that long-range ordering has been destroyed in the presence of quenched heterogeneity, and the system shows the quasi-long-range ordered state. However, results observed for long-range behavior are very much model-dependent. In a recent study, [Kumar et al. (2021)] have found that heterogeneity in the size of active Brownian particles leads to enhanced dynamics. Further, another study by Pattanayak et al. [Pattanayak et al. (2020)] has discussed the effect of heterogeneity in the form of speed of SPPs. They found that the inhomogeneous speed preserves the usual long-range ordering, and induces faster ordering in the system. Besides the studies about active particles in the presence of a different kind of inhomogeneity, there are numerous studies about SPPs in confined geometries. In the ongoing discussion of this thesis, in chapters2, 3, and 4, we discuss some key features of SPPs with respect to their intrinsic inhomogeneous properties.

1.4 Methodology

Non-equilibrium systems are different from their equilibrium counterparts; hence, the methods to characterize their different complex and fascinating behavior are not similar to equilibrium systems. In the non-equilibrium system, there is no conservation of energy;

hence it is not possible to write the effective Hamiltonian to describe such a system. Basically, there are three primary methods to study the active systems in the last few decades described as follows: (i) microscopic rule-based model like the Vicsek model (VM)[Grégoire & Chaté (2004); Vicsek et al. (1995)], and also the derivation of coarse-grained equations for slow variables from the rule-based models[Bertin et al. (2006a); Ihle (2011)], (ii) phenomenological approach which includes writing the different terms in the equations of motion based on the symmetry elements of the system, (iii) and finally, the experiment which provide the realistic features about this systems[Paxton et al. (2004)]. In the next section, we will discuss the details of these studies used in our studies.

1.4.1 Agent or microscopic rule based simulation

Microscopic rule-based modeling is a powerful simulation modeling technique that has seen several applications in the last few years. In agent-based modeling (ABM), a system is modeled as a collection of autonomous decision-making pseudo-particles called agents. Each particle updates its positions and velocities based on the set of fixed dynamical rules. The dynamical rules are adjusted so that they can mimic the phenomenology of the active system. The active particles, which are symmetric in shape, move their long body axis, while for finite-size particles, volume exclusion or steric effects can guide them to align with their neighbors in contact [Chaté et al. (2008); Fily & Marchetti (2012); Pattanayak et al. (2019); Shi & Ma (2013)]. The polar particle interactions can be assumed like "ferromagnetic interaction" in spin systems. Further, for apolar particles, both types of parallel and anti-parallel interactions are possible. In many studies, authors have considered the agents as a point particle but alignment interactions (polar/apolar) are kept by hand to mimic the alignment due to the finite size of the agents [Grégoire & Chaté (2004); Vicsek et al. (1995)]. The interaction among the particles is not always predictable, i.e., the SPPs make errors following their neighbors. These errors are encountered by introducing the noise term in the update equations [Grégoire & Chaté (2004); Vicsek et al. (1995)].

Vicsek Model (VM)

Vicseks' work finds the clustering, transport, and phase transition in the active systems. The original Vicsek model [Vicsek et al. (1995)] is defined in two-dimensions, and is based on the following set of rules: Every SPP in the system is described as a point-particle with a direction $\theta_i(t)$ at time t; the SPP moves along this direction with speed v_0 (often taken equal to 1). At every time step, and for every particle i, there is an alignment rule which works as follows: (i) first one computes the average direction of all particles within a circle $S_i(t)$ centered on the particle position $r_i(t)$ (the i^{th} particle is normally included); (ii) the direction of the particle θ_i is set equal to the angle correspondent to this average direction, plus some noise, which plays the role of rotational diffusion, and shifts stochastically the final direction of an angle by a value randomly chosen in $[-\eta,\eta]$, $\eta \in [0,\pi]$. The equations resulting from the "aligning rule" update at discrete time steps δt, the direction θ_i, the velocity $\mathbf{v_i}$, and the position $\mathbf{r_i}$ as follows:

$$\theta_i(t+\delta t) = arg\Big(\sum_{j\in S_i} e^{i\theta_j}\Big) + \underbrace{\delta\theta_i}_{noise} \tag{1.2}$$

$$\mathbf{v}_i(t+\delta t) = \big(\cos(\theta_i(t+\delta t)), \sin(\theta_i(t+\delta t))\big) \tag{1.3}$$

$$\mathbf{r}_i(t+\delta t) = \mathbf{r}_i(t) + \mathbf{v}_i(t+\delta t)\delta t \tag{1.4}$$

The main reason why the Vicsek model is of interest to the physics of active matter is that it displays a nonequilibrium order-disorder transition when changing the noise strength, η [Chaté et al. (2008); Grégoire & Chaté (2004); Vicsek et al. (1995)]. If the noise is small,

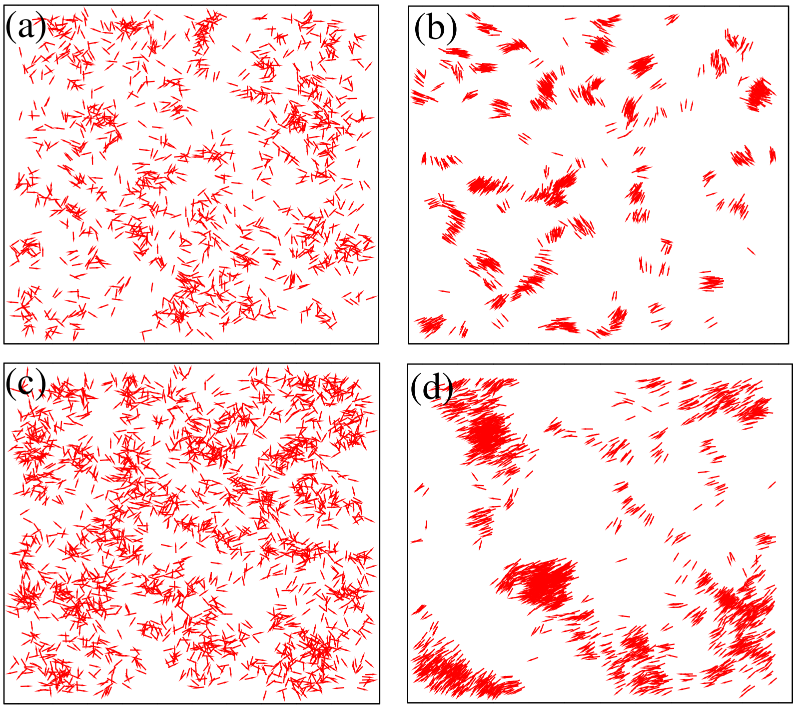

Fig. 1.2 In this figure the velocities of the particles are displayed for varying values of the density and the noise. The actual velocity of a particle is indicated by a small arrow. Four snapshots show the different phases of SPPs with respect to density and noise. (a) At time $t = 0$, $L = 50$, $N = 1340$, $\rho = 0.5$ and $\eta = 0.7$. (b) At time $t = 500$, For small densities and noise the particles tend to form groups moving coherently in random directions, $L = 50$, $N = 1340$, $\rho = 0.5$ and $\eta = 0.2$(c) After some time at higher densities and noise the particles move randomly with some correlation $L = 100$, $N = 2430$, $\rho = 1.0$ and $\eta = 0.7$. (d) For higher density and small noise, the motion becomes ordered $L = 100$, $N = 2430$, $\rho = 1.0$ and $\eta = 0.2$. All of our results shown in Figs.(a)-(d) were obtained from simulations in which velocity $v = 0.5$.

particles tend to align, driving the whole system into an ordered flocking state. For large η , on the other hand, noise prevails, and particles move essentially independently; there is no macroscopic order as shown in Fig.1.2. They also note that for angular noise, the nature of the order-disorder transition becomes discontinuous provided one considers large enough system size because the finite- size effect is much more dominant for angular noise [Foffano et al. (2012)] as compared to the vectorial noise [Grégoire & Chaté (2004)]. The nature of the phase transition in these systems is still a topic of debate. In various studies, the nature of the transition depends on the update mechanism of the system [Aldana et al.

(2007)]. Now, it is believed that the density phase separation is the key to make the transition first order [Pattanayak & Mishra (2018); Solon et al. (2015b)]. But there is still a lack of experiments to settle the debate about the nature of the phase transition. The order parameter which is usually defined to describe this nonequilibrium phase transition is the following:

$$\langle |\mathbf{v}| \rangle = \frac{|\sum_{i=1}^{N} e^{i\theta_i}|}{N} \rightarrow \begin{cases} 1, \eta \to 0 \\ 0, \eta \to 1 \end{cases} \tag{1.5}$$

For $N \to \infty$, the transition has a discontinuous nature [Chaté et al. (2008)], so it is analogous in some respect to an equilibrium first-order transition. In particular, a co-existence of two different phases is observed close to criticality, resulting in the formation of bands [Chaté et al. (2008); Pattanayak & Mishra (2018)], or stripes, which travel along the direction perpendicular to their “axis” (or to the overall tangent to the boundary of the band).

It is instructive to recall that, in the passive limit, where the particles do not move but only align (i.e., the Vicsek model for $v_0 = 0$), the model becomes equivalent (in other words, it lies in the same universality class) to the XY spin model, which displays a Kosterlitz–Thouless phase transition driven by vortex defects unbinding, but not a symmetry-breaking order-disorder transition, like say the Ising model in 2D. This is due to the Mermin Wagner theorem, according to which spins with continuous symmetry, such as the vectors of the XY model, can only undergo an order-disorder transition in a spatial dimension $d > 2$ [Mermin & Wagner (1966)]. On the other hand, the Vicsek particles can exhibit a (symmetry-breaking) order-disorder transition in 2D as well; this is because activity (due to self-propulsion) means that the system is not in equilibrium; hence the Mermin–Wagner theorem does not apply. The Vicsek model also displays other essential and rather generic properties of active systems.

Langevin dynamics for active self-propelled particles

The random motion of particles suspended in a medium (liquid or gas) is known as *Brownian motion*, and the participating particles are referred to as *Brownian or passive particles*. Passive particles continuously suffer collision from their surrounding medium, and their collision dynamics are stochastic. In equilibrium, there is a balance between dissipation and fluctuations in the system, and both of them are related by fluctuation-dissipation relation (FDR) [Pathria (1996); Zemansky & Dittman (1997)]. Dynamics of passive particles described by Newtonian dynamics which includes stochastic and frictional term of forces [Romanczuk et al. (2012)]. Hence, the equation of motion of Brownian particle with Stokes frictional coefficient γ with a position dependent potential $U(r)$ can be written by Langevin dynamics,

$$m\frac{d\mathbf{v}}{dt} = -\gamma\mathbf{v} - \nabla U(\mathbf{r}) + \mathbf{R}(t) \tag{1.6}$$

where **R**(t) is a delta-correlated stationary Gaussian process with mean zero, satisfying the relations $\langle R(t=0)\rangle = 0$, and $\langle R_i(t)\cdot R_j(t)\rangle = 2D_b\delta i, j\delta(t-t')$, where the components $R_i(t)$ and $R_j(t)$ are referred to as Gaussian white noise with intensity D_b. Here indices i and j correspond to the Cartesian coordinates. The intensity D_b and friction coefficient γ are related by the FDR, $D_b = \gamma k_\beta T$ [Pathria (1996); Zemansky & Dittman (1997)] in the equilibrium where k_β and T represent the Boltzmann constant and temperature of the system respectively.

However, ABPs are generally symmetrical in their shape, and hence there is no alignment interaction among them. But the activity of these particles induces motility-induced phase separation(MIPS) [Buttinoni et al. (2013); Cates & Tailleur (2015); van Damme et al. (2019)] at lower density compared to the passive particles. The Langevin equation 1.6 is a second-order stochastic differential equation which includes an inertial term

$m\frac{d\mathbf{v}}{dt}$ and a damping term $\gamma\mathbf{v}$. Generally, in different systems like colloidal suspensions, granular systems, and living organisms, the momentum dissipation caused by the friction is extremely high, such that the motion of ABPs ceases on a very short time. Hence in the mathematical point of view, friction coefficient γ is very large to the mass m. Therefore, the first term of Eq $\sim$ 1.6 can be neglected in the overdamped limit. Hence the dynamics of the ABP in the overdamped regime is given by the following equations:

$$\partial_t \mathbf{r}_i = v_0 \mathbf{n}_i + \mu \sum_{j \neq i} \mathbf{F}_{ij} + \Omega_i^S(t) \tag{1.7}$$

$$\partial_t \phi_i = \Omega(t), \tag{1.8}$$

where ABPs are taken as disk of radius r, and they interect with a soft repulsive potential to take care of steric effects. The direction of motion of the ABP is defined by unit vector $\mathbf{n}_i = \big(\cos(\phi_i), \sin(\phi_i)\big)$, where ϕ_i is the orientation of the i^{th} particle. The first term in the right hand side (R.H.S) of Eq $\sim$1.7 is due to self-propelled nature of the ABP, and v_0 is the self-propulsion speed of the particle. $\Omega_i^S(t)$ shows translational Gaussian white noise with mean zero and correlations $\langle \Omega_{i\alpha}^S(t) \cdot \Omega_{i\beta}^S(t') \rangle = 2D\delta_{ij}\delta_{\alpha\beta}\delta(t-t')$, where α,β denotes Cartesian coordinates and diffusion constant $D = \mu k_\beta T$. $\Omega(t)$ is a rotational Gaussian white noise with zero mean and correlations $< \Omega(t) \cdot \Omega(t') >= 2\Lambda_r \delta_{ij} \delta(t-t')$, Λ_r is the rotational diffusion rate and μ is the mobility. $\mathbf{F}_{ij}$ is short-range repulsive force between i^{th} and j^{th} particle. The nature of soft repulsive potential can be harmonic, Weeks-Chandler-Andersen (WCA), etc. [Fily & Marchetti (2012); Zeitz & Stark (2016)]. It should be taken so that the general properties of the ABPs should be independent of the specific form of the repulsive potential.

1.4.2 Phenomenology : hydrodynamic equations of motion

This subsection is dedicated to the discussion of phenomenological or hydrodynamic equations of motion which are based on symmetry arguments. The discussion involves the flocking model as discussed in section 1.4.1 with the effective continuum theory approach. Effective continuum theory was first proposed by Toner and Tu in 1995 [Toner & Tu (1995, 1998)]. The fundamental principle of hydrodynamic theory includes conservation laws like mass, momentum, and energy conservation, etc. or terms written on the basis of symmetry related to the system. Toner and Tu formulated the effective continuum model on the basis of symmetry considerations. Since the particles move on a frictional dry substrate, and particles continuously dissipates their energy into systematic movement, the only conserved field in the system is the density of active particles $\rho(r,t)$ (excluding death and birth of SPPs). In order to define the different polarisation states of orientation order, one should have to include the dynamics of polarisation vector field $\mathbf{P}(\mathbf{r},t)$. The coarse-grained density $\rho(\mathbf{r},t)$, and polarisation $\mathbf{P}(\mathbf{r},t)$ fields are defined by,

$$\rho(\mathbf{r},t) = \sum_{i=1}^{N} \delta(\mathbf{r} - \mathbf{r}_i(t)) \tag{1.9}$$

$$\mathbf{P}(\mathbf{r},t) = \frac{1}{\rho(\mathbf{r},t)} \sum_{i=1}^{N} \mathbf{n_i} \delta(\mathbf{r} - \mathbf{r}_i(t)) \tag{1.10}$$

where the summation is over all the particles, $\mathbf{r}_i(t)$ and $\mathbf{n}_i(t)$ are the position and the unit orientation vector of i^{th} particle at time t.

Although we are dealing with active systems which are non-equilibrium, it is convenient and instructive to write the dynamical equation of motion arising from a free-energy functional $F(P,\rho)$, where $F(P,\rho)$ includes the interaction among the particles and terms due to activity,

$$\partial_t \rho(\mathbf{r},t) + v_0 \nabla \cdot (\rho \mathbf{P}) = -\nabla \cdot \big(-\frac{1}{\gamma_\rho} \nabla \frac{\delta F(P,\rho)}{\delta \rho} + \mathbf{f}_\rho \big) \tag{1.11}$$

$$\partial_t \mathbf{P} + \lambda_1 (\mathbf{P} \cdot \nabla) \mathbf{P} = -\frac{1}{\gamma} \frac{\delta F(P,\rho)}{\delta \mathbf{P}} + \mathbf{f} \tag{1.12}$$

where γ_ρ, γ are kinetic coefficients, and v_0 is the self-propulsion speed of the active particles. The first term inside the brackets on the right hand side (R.H.S) of Eq $\sim$ 1.11 yields a familiar diffusive current, and $\mathbf{f}_\rho$ is the associated noise. The second term in the left hand side (L.H.S) of Eq $\sim$ 1.11 represents the active current, which is proportional to the self-propulsion speed v_0. Advection present in the system is taken care by considering the advective term of the famous Navier-Stokes equation for fluids. The strength of the advective term in Eq $\sim$1.12 is shown by λ_1 . Unlike the fluid, the nonequilibrium models do not persist in momentum conservation since the particles move on a dissipative substrate and are constrained by Galilean invariance that would need $\lambda_1 = v_0$. But in active flocks, the strength of the advective term λ_1 is a non-universal phenomenological parameter that can be determined from a microscopic model. Here $\mathbf{P}$ denotes both a velocity field and a local orientation order parameter of the system. Therefore, $\mathbf{P}$ introduces a term for advection and flow alignment in Eq $\sim$ 1.12, and $\mathbf{P}$ acts as only a velocity field in Eq $\sim$ 1.11. The last term on the right-hand side (R.H.S) in Eq $\sim$ 1.12 includes the fluctuations in the system, and is a Gaussian white noise with zero mean and correlations such that,

$$\langle f_l(\mathbf{r},t) f_m(\mathbf{r}',t') \rangle = 2\Delta \delta_{lm} (\mathbf{r} - \mathbf{r}') \delta(t - t') \tag{1.13}$$

where Δ is a constant and dummy indices l,m represents Cartesian components. The considered noise in Eqs $\sim$ 1.11, 1.12 is purely additive and does not depend upon order parameter $\mathbf{P}$ and local density ρ. The dual role of $\mathbf{P}$ in the continuum model for active systems as discussed before, **P** plays dual role, (i) **P** is the orientational order parameter of the system, and (ii) $v_0\mathbf{P}$ represents the velocity field. This dual behavior of **P** leads to determine the important large-scale behavior of these systems. Hence, the free-energy functional used in Eqs ∼1.11 and 1.12 is given by

$$F(P,\rho) = \int_r \Big[\frac{\overline{\alpha}(\rho)}{2}|\mathbf{P}|^2 + \frac{\overline{\beta}}{4}|\mathbf{P}|^4 + \frac{\overline{K}}{2}(\partial_l P_m)(\partial_l P_m) + \frac{\omega}{2}|\mathbf{P}|^2\nabla\cdot\mathbf{P} - \omega_1\nabla\cdot\mathbf{P}\frac{\partial\rho}{\rho_0} + \frac{A}{2}\Big(\frac{\delta\rho}{\rho_0}\Big)^2\Big], \tag{1.14}$$

where ρ_0 is the mean density of the system, and $\delta\rho = \rho - \rho_0$ represents the fluctuation in density about its mean value ρ_0. The first two terms of right hand side in Eq ∼1.14 describe the mean-field order-disorder transition of the system. $\overline{\alpha}(\rho)$ is a microscopic model-dependent parameter, which depends on local density ρ and noise strength [Bertin et al. (2006a)]. $\overline{\alpha}(\rho)$ fluctuates around zero near to the critical point, and shows negative value in the ordered state. A reasonable phenomenological method to describe the physics near the transition, where a_0 is a positive constant and $\overline{\alpha}(\rho)$ changes sign at $\rho = \rho_c$. $\overline{\beta}$ shows a positive stablisation factor of the system. In Eq ∼1.14, the third term represents the energy cost due to spatially inhomogeneous deformations of the coarse-grained order $\overline{K}$, and is positive. These order-parameter deformation can arise due to splay or bend parameter, and the Frank constant $\overline{K}$ from splay or bend deformations in two dimensions. The deformations play a significant role in the active systems [Voituriez et al. (2006)]. Further, ω terms can be considered as correction to $\overline{\alpha}(\rho)$ due to splay. The suppression in the density fluctuation is represented by the last term and A shows the compression modulus. Now, using the free energy functional $F(P,\rho)$ of Eq ∼1.14, one can write the hydrodynamic equation of motion of **P** as fallows,

$$\partial_t\mathbf{P} + \lambda_1(\mathbf{P}\cdot\nabla)\mathbf{P} = -\big[\overline{\alpha}(\rho) + \overline{\beta}|\mathbf{P}|^2\big]\mathbf{P} + K\nabla^2\mathbf{P} - v_1\nabla\frac{\rho}{\rho_0} + \frac{\lambda}{2}\nabla|\mathbf{P}|^2 - \lambda\mathbf{P}(\nabla\cdot\mathbf{P}) + \mathbf{f}, \tag{1.15}$$

where $v_1 = \frac{\omega_1}{\gamma}$ and $\lambda = \frac{\omega}{\gamma}$ both represent the dimensions of velocity. Parameters with overline in Eq ∼1.14 are divided by γ and are written without overline in Eq ∼1.15. In polarisation (**P**) Eq ∼1.15 of the polar flock has a fluid character which generally is a function of flock velocity and can be compared to the *Navier-Stokes equation* for a fluid. The second term of the right-hand side of Eq ∼ 1.15 represents the viscous force. The third and fourth term simplify to a pressure gradient gradient $-\frac{1}{\rho}\nabla P$, where considering to the leading order $P(\rho) \approx v_1\rho$ which show the similarity with *Navier-Stokes equation*. Two more important terms based on symmetry argument include hydrodynamic equation for **P** viz; $(\frac{\lambda_3}{2})\nabla|\mathbf{P}|^2 + \lambda_2\mathbf{P}(\nabla$ [(Mishra et al., 2010; Toner & Tu, 1995)]. Derivation of Eqs ∼1.14 and 1.12 $\lambda_3 = -\lambda_2 = \lambda$ based on free energy which has been further derived by [Bertin et al. (2006b, 2009)], and find the relations such that $\lambda_3 = -\lambda_2$, and $\lambda_i \sim v_0^2$, $v_1 = \frac{v_0}{2}$.

1.4.3 Homogeneous steady states

Polar self-propelled particle systems exhibit an order-disorder phase transition, which primarily depends on system parameters like density and noise strength. In a mean-field treatment of homogeneous configuration, one finds a continuous transition from a disordered to an ordered state. The order-disorder transition has been studied using a mean-field treatment in Toner and Tu model [Toner & Tu (1995, 1998)]. Let us consider Eq ∼1.15, in the mean-field approximation, for $\alpha > 0$, corresponds to an equilibrium density $\rho_0 < \rho_c$, the homogeneous steady state of the system is disordered or isotropic, with order parameter $\mathbf{P} = 0$, corresponding to a zero mean velocity. For $\alpha < 0$ corresponding to $\rho_0 > \rho_c$, the system is in the ordered state with a non-zero value of the order parameter, $|\mathbf{P_0}| = \sqrt{\frac{-\alpha_0}{\beta}}$, where $\alpha_0 = \alpha(\rho_0)$, the order moving state, with velocity $\mathbf{v} = v_0\mathbf{P}_0$. The continuous rotational symmetry of the system is spontaneously broken in the ordered state. Further, the advective non-linearities in the hydrodynamic equation of motion of order parameter $\mathbf{P}$ in Eq ∼1.12 establishes long-range ordering in the system even in two dimensions. In the deep ordered state, the linearized hydrodynamics of Eqs ∼1.11 and 1.12 suggests two sound modes, and the propagating sound modes suggest that there exists a symmetry broken state in two dimensions.

1.4.4 Two-point correlations and giant number fluctuations

In active systems, the two important observables are correlation function and structure factor. Using linearized hydrodynamic equations of motion, one can calculate correlation functions and static structure factor $S(\mathbf{K})$ as follows,

$$S(\mathbf{K}) = \frac{1}{\rho_0 V}\langle \delta\rho_{\mathbf{K}}(t)\delta\rho_{-\mathbf{K}}(t)\rangle = \int_{-\infty}^{\infty}\frac{d\omega}{2\pi}S(\mathbf{K},\omega), \tag{1.16}$$

where $\delta\rho_{\mathbf{K}}$ and $S(\mathbf{K},\omega)$ represent the Fourier transform of the density fluctuations, and dynamical structure factor. $S(\mathbf{K},\omega)$ defined as $S(\mathbf{K},\omega) = \frac{1}{\rho_0 V}\int_0^{\infty} dt e^{(i\omega t)}\langle \delta\rho_{\mathbf{K}}(t)\delta\rho_{-\mathbf{K}}(t)\rangle$, where V is the volume of the system, and $\mathbf{K}$, ω are wave vector and angular frequency of the hydrodynamic mode, respectively. $\langle \delta\rho_{\mathbf{K}}(t)\delta\rho_{-\mathbf{K}}(t)\rangle$ gives the density correlation of the system. Toner and Tu show that $S(\mathbf{K}) \sim \frac{1}{K^2}$. The $\frac{1}{K^2}$ divergence at $K \to 0$ reflects a long-wave length fluctuations in the system. The static structure factor $S(\mathbf{K})$ is directly related to the number fluctuation by the relation $\delta N = \sqrt{S(\mathbf{K}\to 0)V}$. The smallest accessible wave vector has $K \sim V^{-\frac{1}{d}}$, where d is the dimension of space. Therefore, $S(K \to 0) \sim V^{2/d} \sim <N>^{2/d}$. Hence active systems show enormous number fluctuation, which is generally referred to as *giant number fluctuations* [Marchetti et al. (2013a)].

1.4.5 Scaling and ordering kinetics

In active matter systems, during the coarsening domains form, and a length scale characterises the morphology of the system [Bray (1994); Puri (2004)]. If the morphology of the domains is statistically invariant with time, and scaling exists in two-point correlation function (density and orientation) then the correlation function can be written as $C(\mathbf{r},t) = g(\frac{r}{L(t)})$, whereas $g(r/L(t))$ is a time-independent scaling function, where $L(t)$ shows the characteristic length of the domain at the time $'t'$. For non-conserved scalar order parameter, the domain of characteristic length L and velocity of domain wall is related to $v \sim \frac{dL(t)}{dt}$, and the curvature of the domain $K \sim \frac{1}{L(t)}$. Hence for the non-conserved scalar order parameter, there is diffusive growth law $L \sim t^{\frac{1}{z}}$ with $z = 2$ (called dynamic exponent) [Bray (1994); Puri (2004)]. For many systems like nematic liquid crystals [Bray (1994); Puri (2004)], we may need n-component vector order parameter. For two components $(n = 2)$ vector order parameter in $2D$ there is logarithmic correction ingrowth law $L(t) \sim (\frac{t}{ln(t)})^{\frac{1}{2}}$ [Bray (1994); Puri (2004)].

For the conserved order parameter systems, the chemical potential μ and domain size $L(t)$ are related to $\mu \sim \sigma/L(t)$, where σ shows the surface tension in the system. Hence there is a concentration current defined by $D|\nabla\mu| \sim D\sigma/L(t)^2$, where D represents the diffusion coefficient. Hence, domain growth is obtained as $L(t) \sim (D\sigma t)^{\frac{1}{z}}$ (z=3) [Glauber (1963)].

1.5 Objective and organisation of this thesis

In the previous sections, we have discussed different classes of the active matter systems based on the system's conservation laws and symmetry elements. We have discussed the general framework to study the active systems and compared them with their equilibrium analogous. We have mentioned the collective behavior and their bulk properties, like order-disorder phase transition, long-range ordering, and phenomenology, etc., of the clean systems [Chaté et al. (2007, 2008); Marchetti et al. (2013b); Ramaswamy (2010b); Vicsek et al. (1995)]. We have mentioned the bulk properties of these systems in the presence of different kinds of heterogeneity which is very often in real systems [Bricard et al. (2013);

Chepizhko & Peruani (2013); Chepizhko et al. (2013); Das et al. (2018); Peruani & Aranson (2018); Sándor et al. (2017); Sándor et al. (2017); Toner et al. (2018a,b)]. We have also discussed the ordering kinetics and steady-state behavior of the active polar systems. With this basic understanding of active matter systems. Next, we will discuss further polar SPPs and ABPs, arranged in the following chapters. In chapter2, we study the phase separation in a binary mixture of self-propelled particles with variable speed. In the ordered state, we find phase separation for two different exponents. Numerical results are also confirmed by the linearized hydrodynamic equations of motion in the ordered state.

In the Vicsek model, the two key assumptions are the polar SPPs moving with the same self-propulsion speed and constant alignment interaction. Still, in natural systems, particles interact differently, depend on their intellectual or physical strength. In the last three decades, many variants of the Vicsek model have been studied to understand various features of different model systems [Chaté et al. (2008); Grégoire & Chaté (2004); Pattanayak & Mishra (2018); Toner & Tu (1998)]. In these studies, authors mainly consider a collection of SPPs in a homogeneous system or medium. Many studies show that inhomogeneity can destroy the LRO present in a disorder-free system [Das et al. (2018, 2020); Singh et al. (2021); Toner et al. (2018a,b)]. In contrast, a few studies discuss special kinds of inhomogeneities that can enhance a system's ordering [Das et al. (2020); Pattanayak et al. (2020)]. Therefore, inhomogeneity can be helpful for many practical applications, e.g., crowd control and faster evacuation, etc. In a recent study, Bialek et al. [Bialek et al. (2012)] show that pairwise inhomogeneous interactions between particles are sufficient to correctly predict the propagation of order throughout the entire flock [Bialek et al. (2012)]. We introduce a collection of polar SPPs with the random-bond disorder, and the particles interact through a short-range alignment interaction. Moreover, the volume exclusion among the particles is taken care of by introducing a repulsive interaction [Caprini et al. (2020); Couzin (2014); Geyer et al. (2019); Sepúlveda et al. (2013)]. The strength of interaction for each particle is obtained from a uniform distribution between $[1-\frac{\varepsilon}{2}:1+\frac{\varepsilon}{2}]$, where ε is the strength of random-bond disorder. For $\varepsilon = 0$, the model represents a disorder-free polar flock with uniform interaction strength for all the particles or the Vicsek-like model [Vicsek et al. (1995)]. Chapter3 and chapter4 are dedicated to studying the role of bond disorder in SPP systems, one away from criticality, and another one near the phase transition. Away from the critical point, we found that the disorder leads to the formation of a random network of different interaction strengths, which makes the alignment weaker and results in slower dynamics and enhanced density clustering. Also, the size of orientationally ordered domains and density clusters grow with time with dynamic growth exponents $z_o \sim 2$ and $z_\rho \sim 4$, respectively. The detailed results are discussed in chapter3.

Near the critical value of noise strength present in the system, the SPPs with bond disorder shows order-disorder transition. The nature of phase transition changes from discontinuous to continuous type by varying the strength of the disorder. The bond disorder also enhances the ordering near the transition due to formation a homogeneous flock state for the large disorder. It leads to faster information transfer in the system and enhances the system's information entropy. This study gives a new understanding of the effect of intrinsic inhomogeneity in the self-propelled particle system. The detailed results are discussed in chapter4.

In chapter5, we study the properties of polar self-propelled particles along a thin junction. Inside the interface (thin junction), particles experience a high noise disordered state, and outside they are in the ordered state. The width of the junction is adjusted by the junction width parameter d. The model is motivated with the Josephson junction [Kontos et al. (2002)], an analogous equilibrium system. The system is studied with and without external perturbation along the direction of the junction. We characterized the system's steady-state behavior and obtained results as follows: (a) Surprisingly, without perturbation, flocks are more ordered comparatively to with perturbation throughout the system. (b) We observe with an increase of the junction width 'd' the amplitude of the orientation current decreases, positive and negative current changes in a periodic fashion with the decrease in the period of current reversal.

In chapter6, we study the phases of passive disk shaped Brownian particles in the presence of potential generated from the system of active Brownian particles. Unlike the equilibrium system, the potential very much depends on the system parameters. A phase diagram is created in the plane of activity and size ratio of active, and passive particles. We observe four distinct phases (1) homogeneous disordered phase (HDP), (2) Homogeneous crystal phase (HCP), (3) Disordered phase-separated phase (DPS), and finally, (4) Ordered phase-separated phase (OPS). Moreover, the system is studied in two ways viz; microscopic and coarse-grain simulation, the observed phases are consistent in both ways. Finally, in chapter7, we conclude the thesis with significant remarks and future prospects of the problems.

1.6 Technical details

The numerical results discussed in the upcoming chapters are obtained by writing the numerical codes and simulated using the FORTRAN 77/90 compiler. Shown figures are generated by using the XMGRACE and GNUPLOT plotting tools. All the simulations are performed at the Institute cluster as well as PARAM SHIVAY computing facility at IIT(BHU) Varanasi India 221005.

****